

Growth of Au Nanowires at the Interface of Air/Water

Zhichuan Xu,^{†,‡} Chengmin Shen,[†] Shouheng Sun,^{*,‡} and H.-J. Gao^{*,†}

Beijing National Laboratory for Condensed Matter Physics, Institute of Physics, Chinese Academy of Sciences, Beijing, China 100190, and Department of Chemistry, Brown University, Providence, Rhode Island 02912

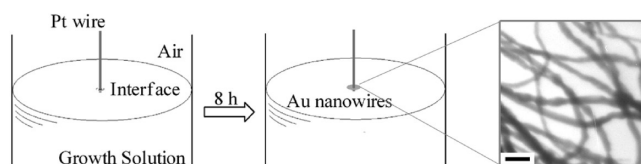
Received: June 9, 2009; Revised Manuscript Received: July 13, 2009

Au nanowires were produced at the interface of air/water by immersing a Au coated platinum tip into the growth solution containing CTAB, HAuCl₄, and ascorbic acid. The Au coating layer is composed of 10–30 nm Au islands and these Au islands initiated the growth of Au crystals, which further produced Au nanowires via the template effect of the aligned cationic surfactant CTAB monolayer at the interface.

Introduction

Nanosized gold (Au) structures are a class of interesting materials¹ for electronic,^{2a} optical,^{2b,c} catalytical,^{2d} and biological applications.³ The wire-like structure (nanowire) is one of the most important Au nanostructures. It exhibits unique surface plasmonic absorptions in two directions^{1a} (longitudinal and transverse) and is capable of serving as a highly efficient electron conductor.^{1c} Extensive studies have been conducted on synthesizing Au nanowires. The favored methods include the reduction of Au³⁺ in anodic aluminum oxide templates and porous membranes,⁴ the solution based reduction of Au³⁺ in the micelles of surfactants such as CTAB⁵ and oleic acid/oleylamine,^{1c,6} and the physical deposition on a patterned substrate.⁷ Recently, synthesizing one-dimensional (1D) nanostructures at the interface have attracted more attention. An interface of air/water or organic/inorganic usually shows polar and nonpolar solubilities at the two sides, which allows the ionic surfactants to form an aligned single molecular layer with their hydrophilic groups wetted in the polar region and hydrophobic groups staying in the nonpolar solvent region.⁸ This property has been utilized to synthesize 1D nanomaterials⁹ in regular micelles and to assemble nanoparticles to a 1D network¹⁰ or ordered packing structures.¹¹ It is known that the cationic surfactant CTAB above critical micelle concentration (CMC) forms not only elongated micelles in a double layer structure in bulk solution⁵ but also a dense aligned monolayer at the interface of air/solution.⁸ Although the former has been intensively studied in a seed-mediated growth procedure to produce 1D Au and Ag nanostructures in bulk solution,^{5,12} the latter has not been reported in producing 1D nanostructures. Actually, these two molecular packing forms of CATB are similar when serving a 1D template, i.e., the ammonium groups coordinate with metal ions and carbon chains align side by side. The problem for producing 1D nanostructures by using such a template at the interface of solution/air is how to initiate the growth of Au crystals at the interface. All the reported methods including seed-mediated,⁵ electrochemical,¹³ and optical¹⁴ initiated the Au crystal growth only in the bulk solution, thus producing 1D Au nanostructures only via double layer structured micelles. In this paper, we report on a method to initiate the Au crystal growth at the interface of solution/air. A microsized platinum tip was coated with a layer

SCHEME 1: Schematic Illustration of Au Nanowire Growth at the Air/Water Interface^a



^a The scale bar of the TEM image is 200 nm. The Au coated Pt tip was immersed into the growth solution containing HAuCl₄, ascorbic acid, and CTAB. After a period of time, the Au nanowires were produced around the Pt tip at the air/water interface.

of Au islands (10–30 nm) in a SEM gold sputter coating apparatus. The Pt tip was immersed into an aqueous solution containing CTAB, HAuCl₄, and ascorbic acid. The nanosized Au islands initiated the growth of Au nanostructures into Au nanowires via the template effect of the aligned CTAB monolayer at the solution/air interface.

Experimental Section

Synthesis. As shown in Scheme 1, HAuCl₄, CTAB, and ascorbic acid were dissolved into deionized water to form a clear light yellow solution of 2 mM HAuCl₄, 0.1 mM CTAB, and 0.5 mM ascorbic acid. The platinum wire was washed with acetone and sequentially ethanol in sonication and dried by nitrogen. The wire was then sputtered with Au in a SEM gold sputter coating apparatus for 30 s. The Au-coated wire was immersed perpendicularly into the 5 mL growth solution with only the tip wetted. The environmental temperature was kept at 30 °C. After 8 h, the solution around the Pt tip area (diameter ~5 mm) changed color to brownish yellow and some solid materials could be observed. The materials were collected by a lab spoon.

Characterization. Samples for TEM were prepared by drying on amorphous carbon coated copper grids and imaged by a JEOL 200CX transmission electron microscope at 120 kV. The X-ray powder diffraction pattern was recorded on a Mac Science M18AHF diffractometer with Cu K α radiation ($\lambda = 1.5418 \text{ \AA}$). The UV–vis spectrum was recorded with a Cary IE spectrometer. The SEM study was carried out on a XL30 S-FEG field emission type scanning electron microscope. The Raman spectrum was recorded on a Raman system YJ-HR800 with confocal microscopy. The solid state diode laser (785 nm) was used as the excitation source with a laser power of 0.6 mW.

* To whom correspondence should be addressed. E-mail: ssun@brown.edu and hjgao@aphy.iphy.ac.cn.

[†] Institute of Physics, Chinese Academy of Sciences.

[‡] Brown University.

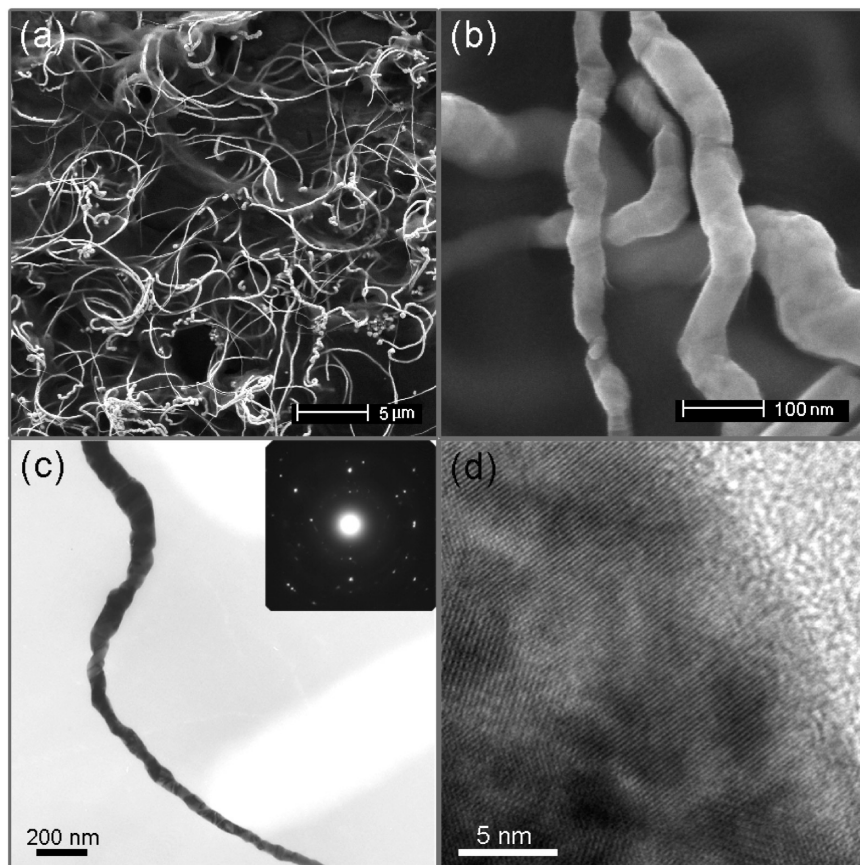


Figure 1. SEM images of as-synthesized Au nanowires at (a) low and (b) high magnification. (c) TEM image of a single wire and its SAED pattern (inset). (d) HRTEM image of a nanowire.

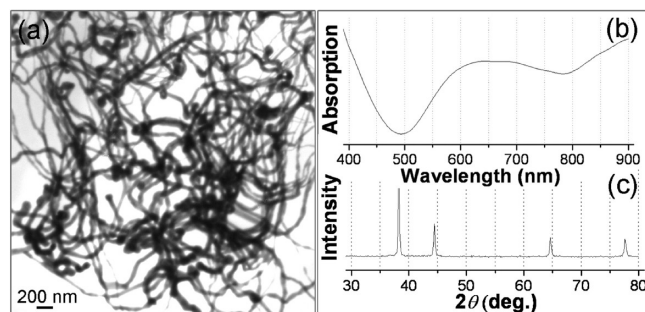


Figure 2. (a) TEM image, (b) UV-vis absorption spectrum of as-synthesized Au nanowires after removing excess CTAB, and (c) XRD pattern.

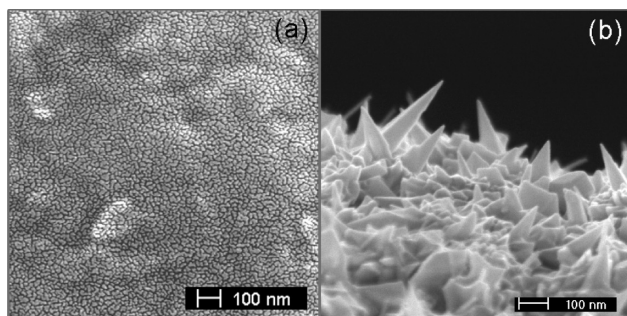


Figure 3. The SEM images of Pt tip surface before (a) and after (b) initiating Au growth.

The Au nanowires were dropped on a cleaned $1 \times 1 \text{ cm}^2$ silicon (111) wafer and dried under ambient conditions. The wafer was immersed into an ethanol solution containing $1 \times 10^{-3} \text{ M}$ 2-naphthalenethiol and then washed with ethanol three times.

Results and Discussion

Figure 1a shows the representative SEM image of as-synthesized Au nanowires. It can be seen that the nanowires extend randomly and build up a cross network. This network is different from the one assembled by Au nanoparticles¹⁰ since the Au nanowires are not connected to each other. A close view of nanowires (Figure 1b) shows that each Au nanowire is an individual structure. The diameter of the nanowires is not uniform and has an obvious size evolution from one end ($\sim 200 \text{ nm}$) to the other ($\sim 50 \text{ nm}$). The length of the nanowires can reach up to $\sim 15 \mu\text{m}$. The cloudy floccule surrounding nanowires is due to the presence of CTAB as a chemical residue after water evaporation and could be confirmed by Br analysis by using the energy dispersive X-ray (EDX) spectrum (Figure S1, Supporting Information). Figure 1c is a typical TEM image of a single Au nanowire. The nanowire surface is not smooth and the twist can be observed. The corresponding selected area electron diffraction (SAED) pattern (the inset) taken from the single nanowire shows random diffraction dots, which indicates that the Au nanowire is polycrystalline. This is further confirmed by HRTEM (Figure 1d), which shows multiple crystal-domain orientations within the 1D structure.

For further characterizations, the Au nanowires were washed with deionized water and centrifuged at 3000 rpm to remove excess CTAB. The Au nanowires were redispersed into deionized water by sonication to form a light pink suspension. Figure 2a shows the TEM image of the Au nanowire suspension. The UV-vis absorption spectrum of Au nanowires (Figure 2b) was recorded right after the suspension was prepared. The Au nanowires exhibit a broad absorption band from 550 to 700 nm as well as an absorption starting at 850 nm. The two broad

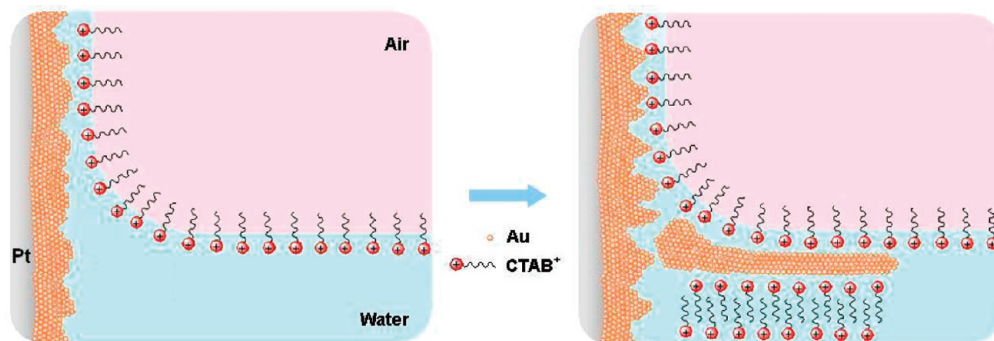


Figure 4. A possible growth mechanism. Au islands initiated the growth of Au crystals at the interface of air/water. The aligned monolayer of cationic surfactant CTAB played the role of template and thus directed the growth of Au nanostructures along one direction.

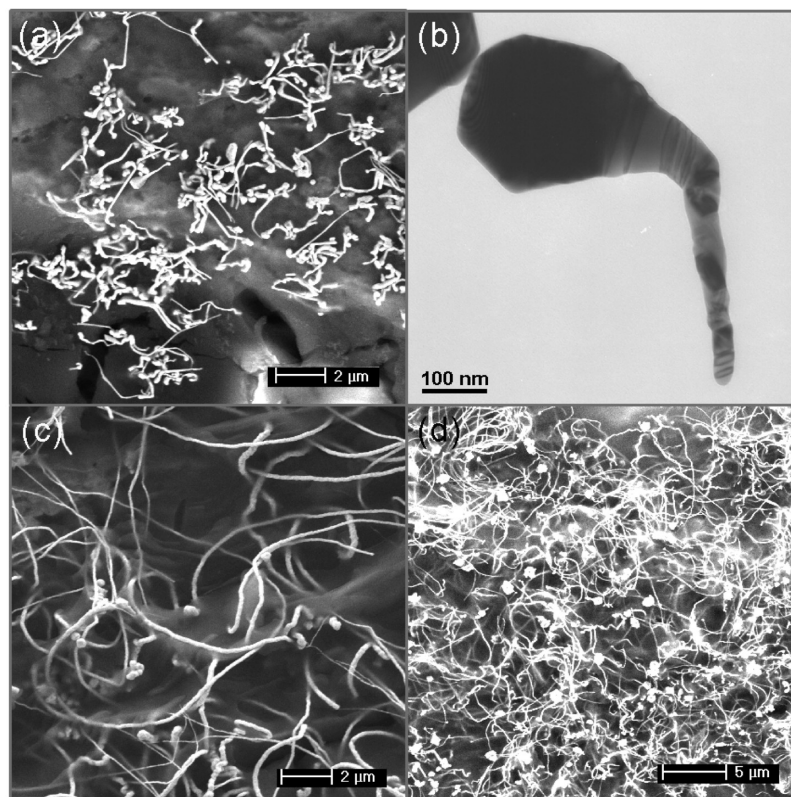


Figure 5. The SEM images of samples at different growth stages: (a) 3, (c) 6, and (d) 8 h. The TEM image of a small tadpole-like particle (b) found in the 3 h sample implies that the growth of nanowires is started from the Au nanocrystals.

absorption characteristics could be ascribed to the transverse and longitudinal absorptions, respectively. Due to the fact that the nanowires have a wide dimension distribution, the absorption bands are wide and the longitudinal one starting at 850 nm should extend to a quite high wavelength region. The tails presented in the spectrum below 450 nm should be ascribed to the interband transition absorption in Au.¹⁵ Figure 2c shows the XRD pattern of as-synthesized Au nanowires. The sample for XRD analysis was prepared by redispersing Au nanowires into 0.5 mL of ethanol and dropping them onto a glass slide. The XRD pattern shows a typical fcc Au crystal phase. The diffraction peaks at 38.2, 44.4, 64.6, and 77.6° correspond to the crystal planes (111), (200), (220), and (311), respectively.

The Pt tip was examined by SEM. Panels a and b of Figure 3 show the SEM images of the Pt tip surface before and after the growth of Au nanowires, respectively. Before initiating Au growth, the surface of the Pt tip was sputtered with a Au layer and this layer has 10–30 nm Au islands densely on its surface. By wetting the Pt tip with the solution, these islands probably

played the role of seeds and initiated the growth of Au nanostructures on the tip surface^{5,16} (Figure 3b). The growth that took place at the solution/air interface was mainly templated by the aligned monolayer of CTAB, as illustrated in Figure 4, and thus the crystals grow along one direction to form nanowires. The CTAB monolayer stabilizes one side of the Au nanowires and the other sides should be surrounded by the CTAB double layered structures, which is the typical structure of CTAB in bulk solution.⁵ This probably is the reason that the process produced nanowires rather than a sheet structure. As the size of the nanowires increased, they separated from the tip surface and were suspended at the solution/air interface by surface tension, probably followed by further growth. The growth took place in bulk solution resulting in a small number of large Au nanostructures with various shapes (Figure S2, Supporting Information) and these nanostructures are precipitated out at the bottom of the solution due to their gravity.

To further investigate the growth process, the samples at different stages were collected and observed by SEM. Figure 5

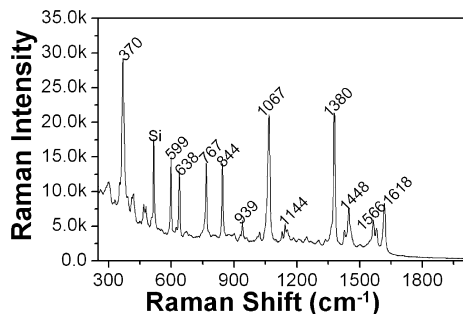


Figure 6. The SERS spectra of 2-naphthalenethiol adsorbed on the as-prepared Au nanowires at an excitation source of 785 nm.

shows the SEM images of samples collected at 3, 6, and 8 h growth periods. At the earliest stage, short nanowires ($\sim 2 \mu\text{m}$ in length) could be found, each with a tadpole-like shape (Figure 5a). A close view of a small tadpole-like particle by TEM shows clearly the tail extends from the main body of the crystal (Figure 5b). This implies that the growth of nanowires probably was started from Au islands, and further selectively depositing Au onto the particle surface with the assistance of CTAB⁺ surfactant molecules led to a prolongation of nanoparticles along one direction.⁵ The monolayer of surfactant CTAB⁺ at the interface probably played the role of a large-sized soft template and facilitated the growth of Au nanowires at the interface (Figure 4). This is much bigger than the soft template for the growth of Au nanorods, which is usually in the size range of CTAB micelles.⁵ The tadpole-like nanowires extended their tails as the growth time increased and the length of nanowires became longer. In 6 h, the nanowires extended their length to over $8 \mu\text{m}$ (Figure 5c). After 8 h of growth, the length of the nanowires reached up to $\sim 15 \mu\text{m}$. In Figure 3d, it can be seen that Au nanowires finally formed a cross network, which indicates the growth of Au nanowires takes place in a high density and the nanowires are intertwined with each other during the growth. The observation of samples at each growth stage reveals that the growth of Au nanowires starts with Au islands followed by a continuous depositing of Au on the crystals in the presence of CTAB⁺ at the interface. It should be noticed that as long as the Au nanowires departed from the Pt surface region, the bare Au island surface was available again for initiating the growth of new Au crystals. Therefore, initiating the growth of Au nanowires by Au islands is a continuous phenomenon and the product is always a mixture of fully grown Au nanowires and newly produced ones, which should be the main reason why the length of Au nanowires is not uniform. A control experiment was also carried out to confirm the function of Au islands. A bare Pt tip without the Au islands coating was immersed into the growth solution. The growth of Au nanowires at the interface was hardly initiated. However, by aging for enough time (over 1 day) some large Au crystals can be found at the bottom of the container (Figure S3, Supporting Information). The details for how the growth of these Au crystals in bulk solution is initiated are not clear. But probably it is due to the curved electric double layer formed around the Pt tip,^{5d,17} which probably induced potential redistribution and facilitated the reduction of Au⁺-CATB to small crystals, and these small crystals further grow to big crystals.¹⁸ The control experiment indicates that the Au island coating layer is essential for the growth of Au nanowires at the interface of solution and air.

The as-prepared Au nanowires were used for the surface-enhanced Raman scattering (SERS). The Au nanowires were dried on a cleaned silicon wafer and immersed into an ethanol solution containing 1×10^{-3} M 2-naphthalenethiol. The wafer

was then washed with ethanol and dried under ambient condition. Figure 6 shows that the SERS spectrum of 2-naphthalenethiol adsorbed on Au nanowires at an excitation source of 785 nm. The vibrational modes of C–S and C–C can be seen clearly at 370, 1067 cm^{-1} , and 1380, 1618 cm^{-1} , respectively.^{2c,19} The peaks at 599 and 638 cm^{-1} correspond to ring deformation.^{19d} The C–H wag and twist can be seen at 767 and 844 cm^{-1} . The S–H bend at 939 cm^{-1} , the ring stretch at 1566 cm^{-1} ,^{19d} and the b_2 modes located at 1144 and 1448 cm^{-1} are also enhanced to be visible, indicating that the Au nanowires are very SERS active.¹⁷

Conclusions

In summary, a unique growth process of Au nanowires in the air/water interface is presented in this paper. By wetting a Au coated platinum tip into the growth solution containing CTAB and HAuCl₃, the Au nanowires can be produced around the region close to the Pt tip. The growth of nanowires is facilitated by the CTAB template at the air/water interface. This approach offers an alternative method for growing 1D Au nanostructures for optical and electronic applications.

Acknowledgment. The work was supported by the National Science Foundation of China (grant nos. 50872147 and U0734003) and the CAS/SAFEA international cooperation team.

Supporting Information Available: EDX spectra of Au nanowires and SEM image of Au particles produced in bulk solution. This material is available free of charge via the Internet at <http://pubs.acs.org>.

References and Notes

- (1) (a) Link, S.; El-Sayed, M. A. *J. Phys. Chem. B* **1999**, *103*, 8410. (b) Aherne, D.; Satti, A.; Fitzmaurice, D. *Nanotechnology* **2007**, *18*, 125205. (c) Wang, C.; Hu, Y.; Lieber, C. M.; Sun, S. *J. Am. Chem. Soc.* **2008**, *130*, 8902.
- (2) (a) Quin, L.; Park, S.; Huang, L.; Mirkin, C. A. *Science* **2005**, *309*, 113. (b) Wohltjen, H.; Snow, A. W. *Anal. Chem.* **1998**, *70*, 2856. (c) Shen, C.; Hui, C.; Yang, T.; Xiao, C.; Tian, J.; Bao, L.; Chen, S.; Ding, H.; Gao, H. *Chem. Mater.* **2008**, *20*, 6939. (d) Hammer, B. *Top. Catal.* **2006**, *37*, 3.
- (3) (a) Han, M. S.; Lytton-Jean, A. K. R.; Mirkin, C. A. *J. Am. Chem. Soc.* **2006**, *128*, 4954. (b) Huang, X.; El-Sayed, I. H.; Qian, W.; El-Sayed, M. A. *J. Am. Chem. Soc.* **2006**, *128*, 2115.
- (4) Wirtz, M.; Martin, C. R. *Adv. Mater.* **2003**, *15*, 455.
- (5) (a) Jana, N. R.; Gearheart, L.; Murphy, C. J. *J. Phys. Chem. B* **2001**, *105*, 4065. (b) Nikoobakht, B.; El-Sayed, M. A. *Chem. Mater.* **2003**, *15*, 1957. (c) Johnson, C. J.; Dujardin, E.; Davis, S. A.; Murphy, C. J.; Mann, S. *J. Mater. Chem.* **2002**, *12*, 1765. (d) Perez-Juste, J.; Liz-Marzan, L. M.; Carnie, S.; Chan, D. Y. C.; Mulvaney, P. *Adv. Funct. Mater.* **2004**, *14*, 571. (e) Xu, Z.; Shen, C. M.; Xiao, C. W.; Yang, T. Z.; Zhang, H. R.; Li, J. Q.; Ki, H. L.; Gao, H. *J. Nanotechnology* **2007**, *18*, 115608.
- (6) (a) Halder, A.; Ravishanker, N. *Adv. Mater.* **2007**, *19*, 1854–1858. (b) Huo, Z.; Tsung, C.; Huang, W.; Zhang, X.; Yang, P. *Nano. Lett.* **2008**, *8*, 2041. (c) Lu, X.; Yavuz, M. S.; Tuan, H. Y.; Korgel, B. A.; Xia, Y. *J. Am. Chem. Soc.* **2008**, *130*, 8900. (d) Pazos-Perez, N.; Baranov, D.; Irsen, S.; Hilgendorff, M.; Liz-Marzan, L. M.; Giersig, M. *Langmuir* **2008**, *24*, 9855.
- (7) Calleja, M.; Tello, M.; Anguita, J.; Garcia, F.; Garcia, R. *Appl. Phys. Lett.* **2001**, *79*, 2471.
- (8) (a) Lopez-Garcia, J. J.; Aranda-Rascon, M. J.; Horno, J. *J. Colloid Interface Sci.* **2007**, *316*, 196. (b) Loeb, A. L. *The electrical Double Layer Around a Spherical Colloid Particle*; Massachusetts Institute of Technology Press: Boston, MA, 1961.
- (9) (a) Tang, J.; Cui, X.; Liu, Y.; Yang, X. *J. Phys. Chem. B* **2005**, *109*, 22244. (b) Song, X.; Sun, S.; Zhang, W.; Yu, H.; Fan, W. *J. Phys. Chem. B* **2004**, *108*, 5200.
- (10) Ramanath, G.; D'Arcy-Gall, J.; Maddanimath, T.; Ellis, A. V.; Ganesan, P. G.; Goswami, R.; Kumar, A.; Vijayamohan, K. *Langmuir* **2004**, *20*, 5583.
- (11) Gattas-Asfura, K. M.; Constantine, C. A.; Lynn, M. J.; Thimann, D. A.; Ji, X.; Leblanc, R. M. *J. Am. Chem. Soc.* **2005**, *127*, 14640.

(12) Jana, N. R.; Gearheart, L.; Murphy, C. J. *Chem. Commun.* **2001**, 617.

(13) Yu, Y. Y.; Chang, S. S.; Lee, C. L.; Wang, C. R. C. *J. Phys. Chem. B* **1997**, *101*, 6661.

(14) Esumi, K.; Matsuhisa, K.; Torigoe, K. *Langmuir* **1995**, *11*, 3285.

(15) Alvarez, M. M.; Khoury, J. T.; Schaaff, T. G.; Shafiqullin, M. N.; Vezmar, I.; Whetten, R. L. *J. Phys. Chem. B* **1997**, *101*, 3706.

(16) Taub, N.; Krichevski, O.; Markovich, G. *J. Phys. Chem. B* **2003**, *107*, 11579.

(17) (a) Pakarinen, O. H.; Foster, A. S.; Paajanen, M.; Kalinainen, T.; Katainen, J.; Makkonen, I.; Lahtinen, J.; Nieminen, R. M. *Modell. Simul. Mater. Sci. Eng.* **2005**, *13*, 1175. (b) Marmur, A. *Langmuir* **1993**, *9*, 1922.

(c) Israelachvili, J. N. *Intermolecular and Surface Forces*; Academic: London, UK, 1991.

(18) Yu, Y. Y.; Chang, S. S.; Lee, C. L.; Wang, C. R. C. *J. Phys. Chem. B* **1997**, *101*, 6661.

(19) (a) Zheng, J.; Li, X.; Gu, R.; Lu, T. *J. Phys. Chem. B* **2002**, *106*,

1019. (b) Osawa, M.; Matsuda, N.; Yoshii, K.; Uchida, I. *J. Phys. Chem.* **1994**, *98*, 12702. (c) Nikoobakht, B.; El-Sayed, M. A. *J. Phys. Chem. A* **2003**, *107*, 3372. (d) Alvarez-Puebla, R. A.; Dos Santos, D. S., Jr.; Aroca, R. F. *Analyst* **2004**, *129*, 1251.

JP905396R